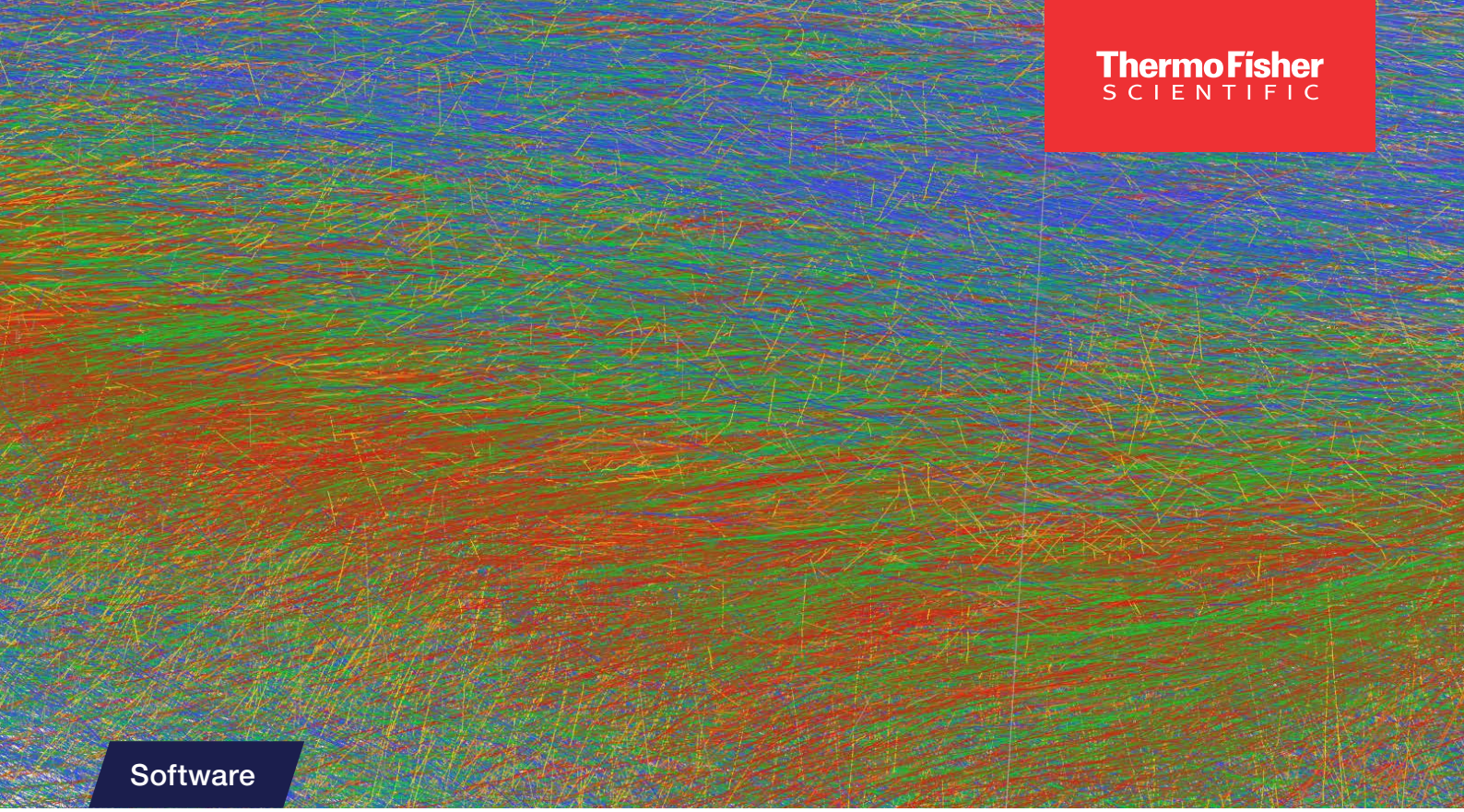

Software

Comparison of fiber orientation analysis methods

Authors

Rémi Blanc[1], Peter Westenberger[2]

1,2 Thermo Fisher Scientific

Keywords

Fiber Analysis, Quantification, Orientation, Distribution

Abstract

Computed Tomography (CT) is on its way to become the de facto standard in the field of materials science and material development especially when it comes to the analysis of fibrous materials. It provides full 3D details inside the materials, and enables non-destructive analysis, which may be coupled with either in-situ experiments or numerical simulations to assess the physical properties of the materials. The current question is mostly about the compromise between image resolution and volume

of data being analyzed, to extract accurate information allowing for the characterization of the fibrous material. Among those statistics, we focus here particularly on the distribution of fiber orientations within the material. We will highlight three different approaches that may operate at different resolutions to provide insights about the fiber orientations.

After presenting these different methods in a first part, we will then describe the data used for this study. We will apply the described procedures to real data that has been acquired by a state of the art µCT system. We will also work with an artificial dataset generated with user-defined properties, which provides us with a goldstandard reference against which the result methods can be evaluated. For both real and synthetic data, we will also investigate the behavior of the proposed approaches with respect to the scanning resolution, simulated here by applying them on down-sampled versions of the same original images. The obtained results will be presented in section 3, allowing us to draw conclusions on the respective merits of the proposed estimation methods.

thermo scientific

1. Methods

We consider three different methods for estimating the local fiber orientation, in sub-volumes of predefined size and positioned without overlap along a regular lattice. The first approach (FFT) is based on the principal component analysis of the Fourier Spectrum, inspired from [1]. The second approach (GRAD) relies on the analysis of the local gradients [2]. These first two approaches rely on the texture of the image to derive estimates of the local orientation, and are expected to provide results even in the case of low resolution data where individual fibers cannot be distinguished. The third method (XFIBER) consists in segmenting each individual fiber and extracting their centerlines, which gives immediate access to all statistics regarding orientations of the fibers, but also length, diameter or even tortuosity of fibers. The approach, described in [3,4], relies on a template matching stage and a specific fiber tracing algorithm. All three methods are implemented in Avizo 3D software for scientific and industrial data developed by Thermo Fisher Scientific.

The methods are configured to operate on the same subdivisions of the data, to generate a tensor representing the local distribution of orientations in the corresponding subvolumes. This tensor is symmetric positive in all three cases, and its eigenvalue decomposition provides insights about the major orientation, and the dispersion of orientations. In the XFIBER approach, which relies on explicitly detected fibers, the orientation tensor is clearly interpretable [5]. It is defined as the outer product of unit vectors representing the orientation of fiber segments, weighted by the corresponding segment length L, and normalized such that they have unit trace:

$$A = k \sum L_i \vec{u}_i \cdot \vec{u}_i^T$$

In contrast, the FFT and GRAD derive their tensors from image texture descriptors, making their interpretation less straightforward, and a direct comparison challenging.
For instance, in the FFT approach, the major orientation corresponds to the direction where there is the least amount of high frequency variations, and thus to the eigenvector corresponding to the lowest eigenvalue. On the contrary, for the GRAD and XFIBER approaches, the major orientation is the eigenvector corresponding to the largest eigenvalue.

Therefore, we rather perform our comparisons of the methods based on the statistical relationship between the estimated tensors, and on the estimated major orientation.

2. Data sources

2.1 Generation of synthetic data

A synthetic distribution of non-overlapping fibers (straight cylinders) following a skin-core structure has been generated, such that the different methods for estimating the fiber orientations may be compared quantitatively against a known reference. The synthesis has been performed using a force-biased algorithm inspired from [6]. The process starts with the insertion of fibers following prescribed random distribution laws for their position, length, orientation and diameter, within the volume of interest. Then, the algorithm iteratively translates and rotates fibers that are overlapping. The diameter of all fibers is also slightly reduced at each iteration to ensure the convergence of the algorithm. A fiber volume fraction around 10% was obtained. The volume was discretized, including moderate gaussian noise and blurring, with a resolution such that the average fiber diameter corresponds to 5 voxels, and turned into a grayscale image of 512x512x512 voxels as illustrated in Figure 1.

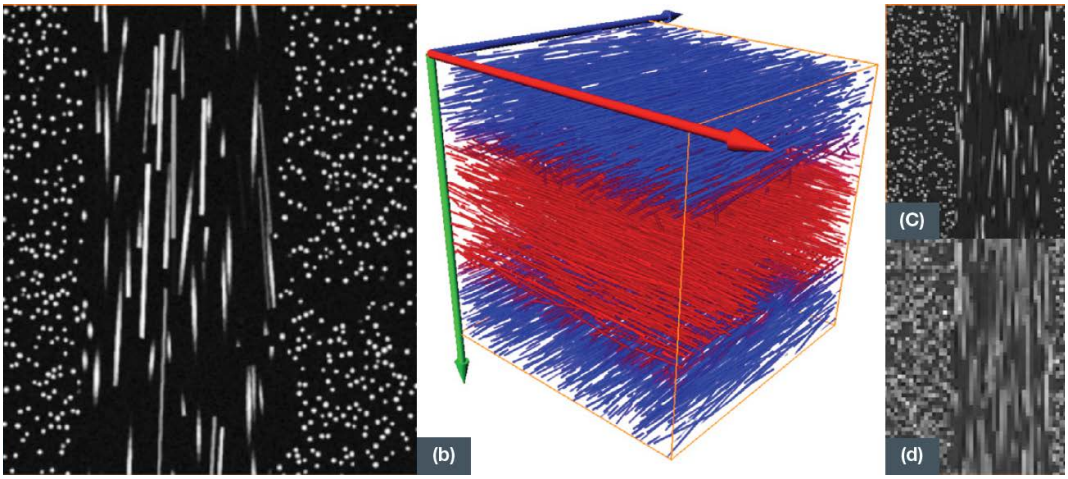

Figure 1: (a) Slice through the synthetic volume, (b) 3D volume rendering of the synthetic volume, colorized according to the estimated major orientation (the red, green and blue axes indicate the color code), (c) slice through the synthetic volume, downsampled by a factor 4, (d) downsampled by a factor 8.

2.2 Glass fiber composite

We also apply the methods on an actual µCT acquisition of a Glass Fiber Reinforced Polymer (GFRP), shown in Figure 2. The polymer is charged with standard short glass fibers of 10µm diameter on average, at a volume fraction measured around 17% in the considered volume of interest, which is roughly 2x2x2mm^3. The scanning resolution is 1.5µm, which is sufficient to distinguish individual fibers.

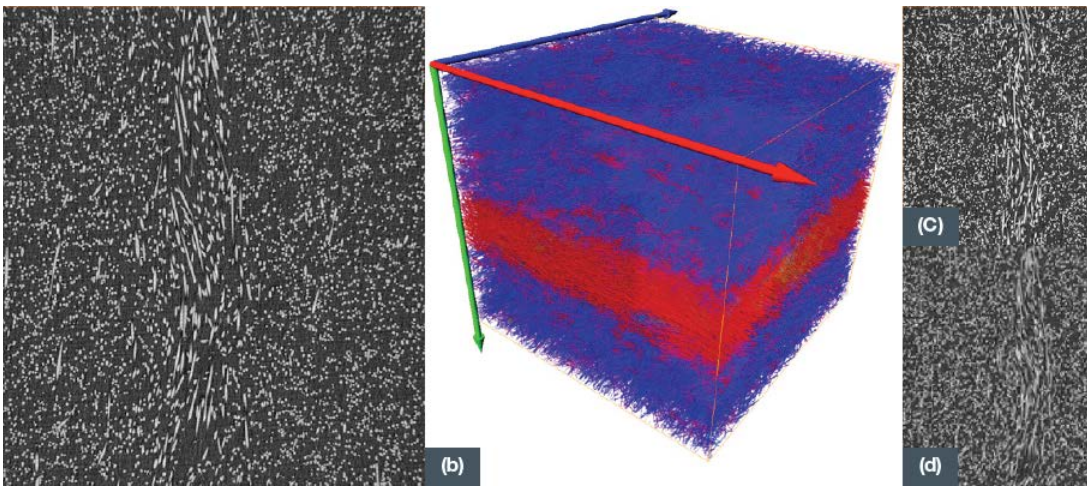

Figure 2: (a) Slice through the GFRP volume, (b) 3D volume rendering of the GFRP volume, colorized according to the estimated major orientation (the red, green and blue axes indicate the color code), (c) image downsampled by a factor 4, and (d) factor 8.

3. Results

The volumes are subdivided in cubic regions following a regular lattice, to perform local orientation analyses using all three methods. Both datasets follow a similar skin-core structure with orthogonal fiber orientations. The subdivision of both volumes is made such that most slabs of the data contain homogeneous regions in terms of fiber orientation with one clear major orientation (either X or Z), while other slabs contain a mixture of fibers oriented mostly along X, and along Z. For both datasets, the local orientation was measured on the full resolution data, but also after downsampling by a factor 4, and 8, using Lanczos interpolation, to evaluate the robustness of the estimates with respect to imaging resolution.

3.1 Synthetic data

For the synthetic dataset, we compute the reference orientation tensor using (eq. 1), i.e. the same approach as with XFIBER, although on the true fiber segment (before discretization), whereas the XFIBER measure is generated after generating a grayscale volume and performing the fiber detection on it. Considering the whole volume, the different approaches show strong statistical relationships with the reference tensors, which seem almost linear as can be seen in Figure 3. The coefficient of determination R^2 appears to be very strong, except for the diagonal component in the GRAD approach. This tendency is fairly well maintained when decreasing the image resolution, as shown in Figure 3(d). The off-diagonal component appear more difficult to estimate, and less robust. However, it must be noted that in the considered synthetic model, few fibers are actually significantly away from the two major orientations, making it more difficult to draw conclusions. It seems more interesting to note that, although the actual accuracy of the fiber detection of the XFIBER approach considerably drops at lower resolution, the results of the tracing still show high value in terms of orientation measurements.

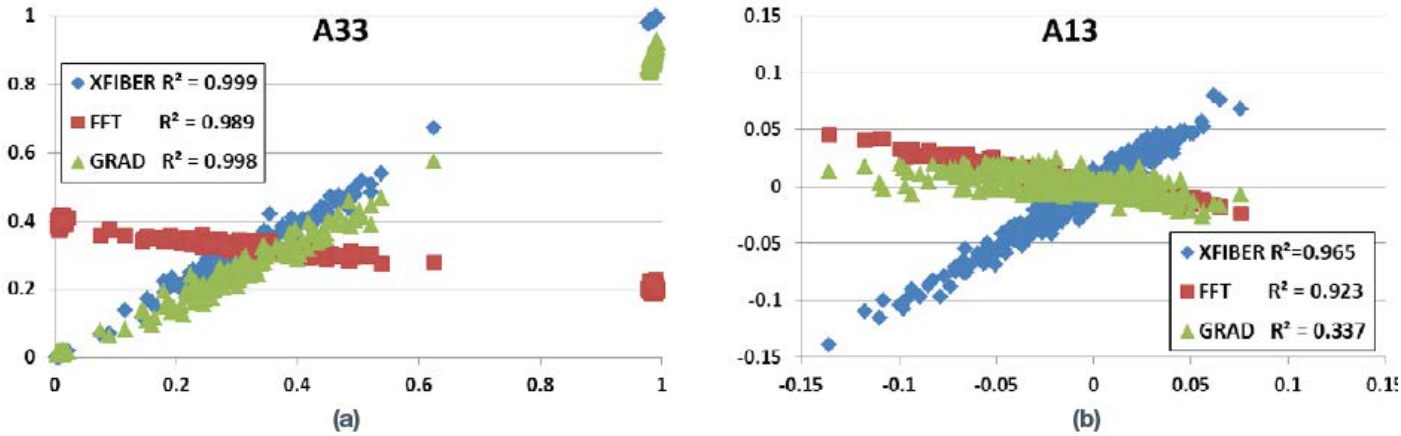

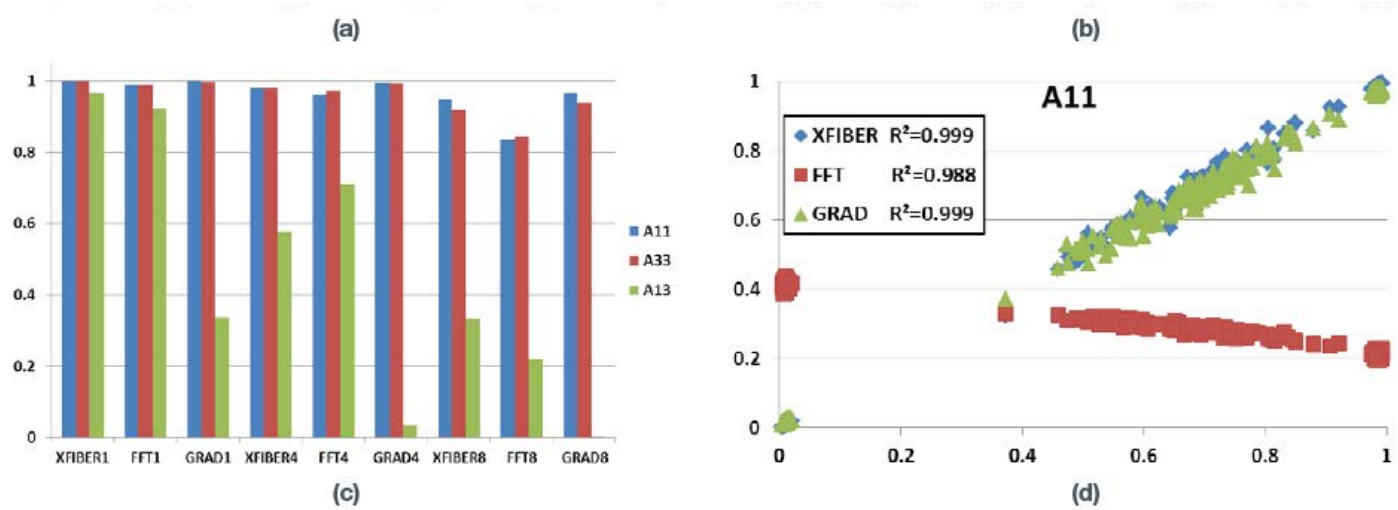

Figure 3: (a), (b), (c) Scatter plots of the true vs estimated tensor components, respectively (a) A11, (b) A33, and (c) A13. (d) Corresponding coefficients of determination for the tensor components, estimated using the different methods at different image resolution.

Examining the results slab by slab, through the thickness of the data structure, allows us to investigate results in more details. The subdivision of the data has been performed such that all slabs except slab 3 and 6 present homogeneous population of fibers which are oriented either along the X (slabs 4 and 5) and Z (slabs 1, 2, 7 and 8) axes, whereas slabs 3 and 6 contain a mixture of fibers oriented in X and Z directions (about 2/3 of fibers are along X, and 1/3 along Z). This is visible in Figure 4(a).

In homogeneous regions (all slabs except 3 and 6), the average angular error (angle between the true major orientation, and the estimated orientation) was very low for all 3 methods, with respectively 0.35, 0.48 and 1.26 degrees for the XFIBER, FFT and GRAD.

On the other hand, in inhomogeneous regions (slabs 3 and 6), the estimation of the major orientation proved to be prone to significant errors using texture-based approaches, whereas the fiber tracing approach remained very precise. However, as can be seen on Figure 4(b), the estimation is significantly more accurate and robust with respect to resolution using the XFIBER approach compared to the texture-based measurement methods GRAD, and especially FFT.

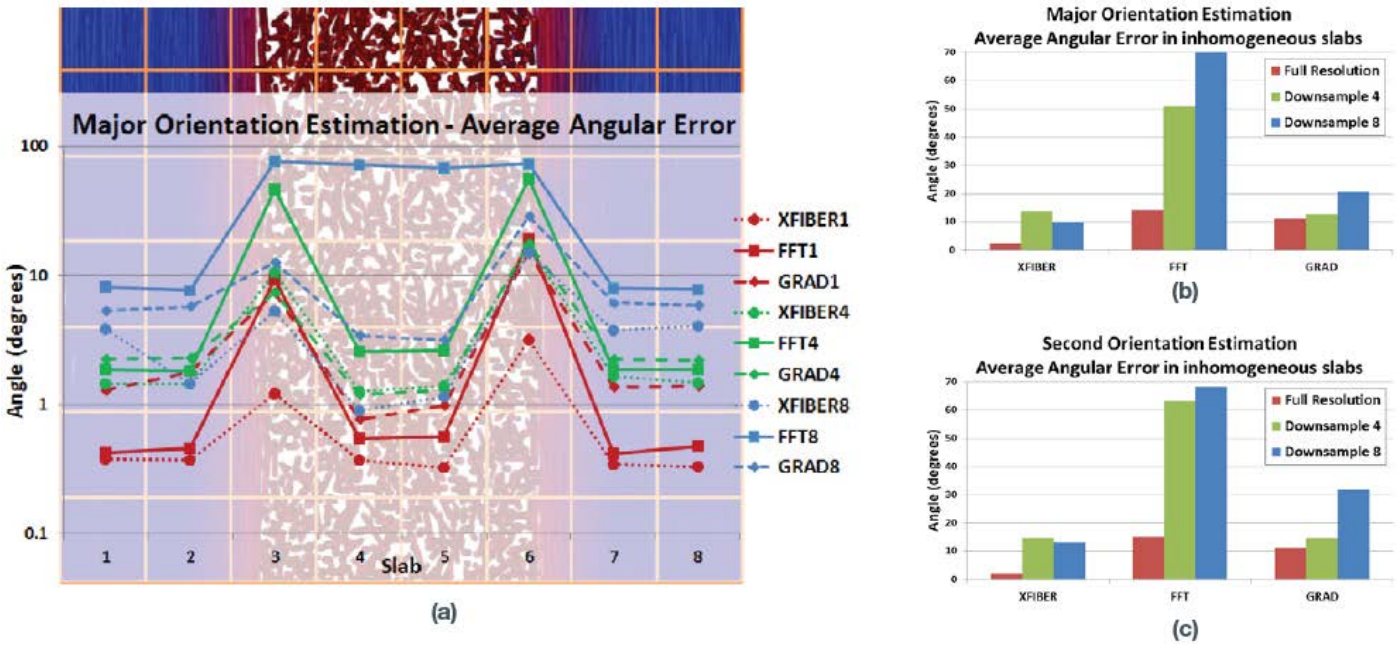

Figure 4: (a) Representation of the subdivisions for local orientation analysis, and plot of the average angular error in the estimation of the major orientation using each 3 method. The errors are averaged per slabs, a logarithmic scale is used for the angular error. (b) Average angular error for the major, and (c) second orientations within slabs 3 and 6, which presents two populations of fibers.

3.2 Glass fiber composite

A similar experiment and analysis was carried out on the GFRP sample. Since no ground truth orientation measurements are available in this case, we use the results generated by the XFIBER method at full resolution as a reference. The results are presented in Figure 5.

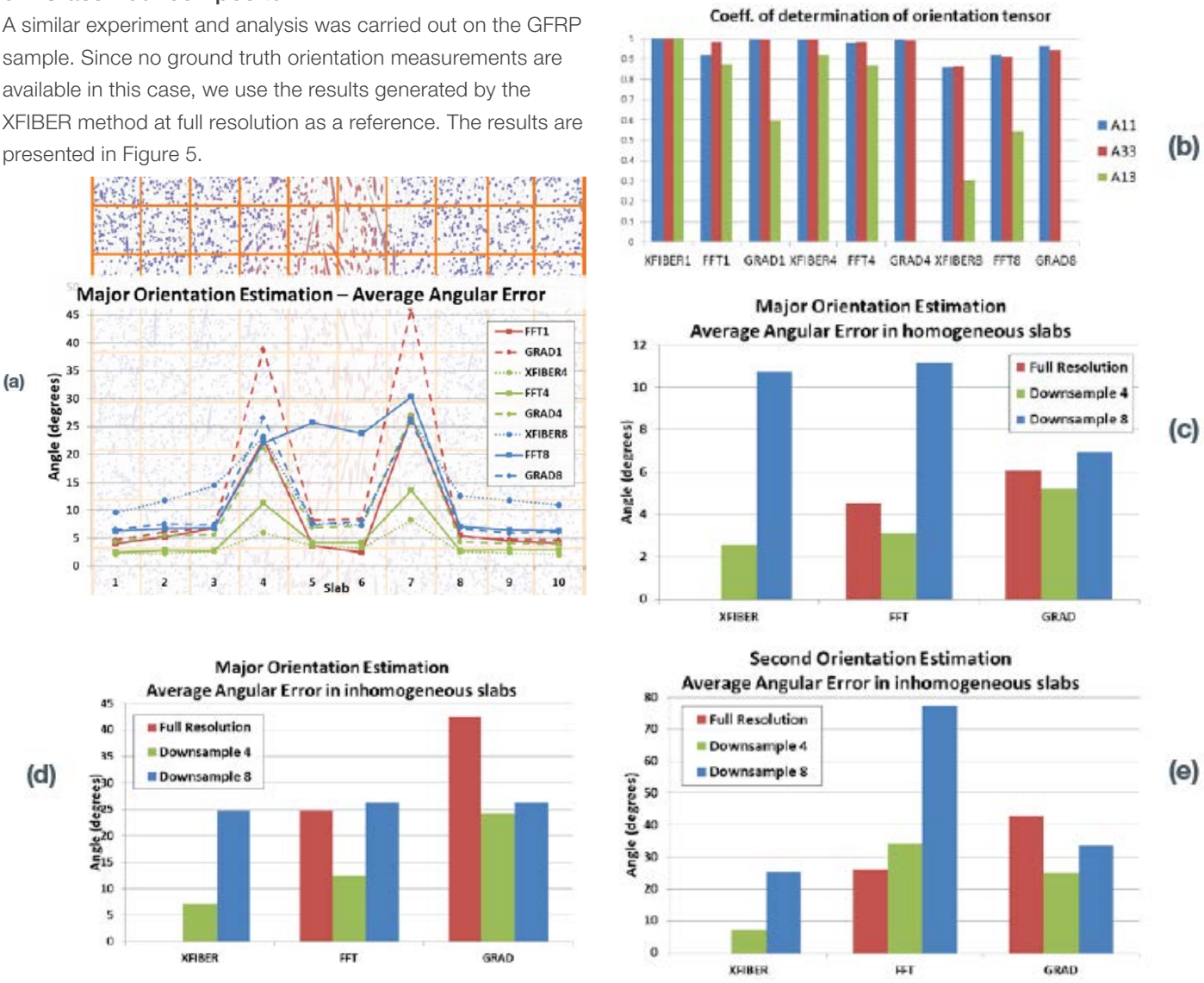

Figure 5: (a) Representation of the subdivisions for local orientation analysis, and plot of the slab-averaged angular error in the estimation of the major orientation using each 3 method at the different resolutions. The reference measurement is the result of XFIBER1. (b) Coefficients of determination for the tensor components (b) Average Angular Error for the estimation of the major orientation, within slabs with homogeneous orientations (all but slabs 4 and 7). (d) Average angular error for the major, and (e) second orientations within slabs 4 and 7, which clearly present two populations of fibers.

As with the synthetic dataset, and when considering volume-wise statistics, the different methods appear to be very strongly correlated. The coefficients of determination of the tensor components are very high (Figure 5(b)), and the major orientation estimation remains within 5 degrees in homogeneous regions of the data, and still within 12 degrees after downsampling by a factor of 8.

However, the estimations from the different methods vary significantly when considering inhomogeneous slabs 4 and 7, which are at the interface between regions presenting orthogonal fiber directions. Although the XFIBER approach provides estimated orientation that are relatively consistant across scales (<10° difference for the major and second orientation at resolution factor 4), the other methods show considerably more deviations (around 20° or more).

4. Conclusion

We presented and compared three different approaches aiming at the estimation of local fiber orientation statistics within composites, based either on texture-based measures, or on the explicit detection and tracing of individual fibres. These approaches, implemented in the Avizo software, have been applied on a skin-core glass-fiber reinforced polymer, and on a synthetic dataset generated with a similar fibrous structure providing a gold-standard reference. We also investigated the robustness of the estimates with respect to decreasing
the image resolution, as the typical practical tradeoff with CT acquisition, is to choose between imaging smaller volumes at a higher magnification, or using a coarser resolution but increased volume of acquisition.

The results on both synthetic and real data suggest that the fiber local orientation tensor estimations are, overall, quite consistent for the different methods, and relatively robust to a decrease of the image resolution. Interestingly, even if in terms of detection performance, the fiber tracing accuracy drops significantly when the image resolution reaches the fiber diameter, the results it generates are still exploitable, and actually quite precise and robust to characterize the orientations in the sample.

The fibre architecture considered in this study allows us to analyse regions with a single population of fibers, all more or less oriented along the same orientation; as well as regions featuring two populations of fibres with two orthogonal preferred orientations. When a single orientation is present, although
the fiber tracing approach is slightly more precise especially at finer resolutions, all considered methods behave accurately. However, when a mixture of orientations are present, the texture-based approaches show significantly decreased performances, whereas the fiber tracing approach remains precise, even at relatively coarse image resolution. This is particularly interesting when considering fibrous materials exhibiting complex distributions of orientations, such as woven fibres, moulded composites, or more random distributions.

References

[1] Bigün et al. (1987). Optimal orientation detection of linear symmetry, in Proc. ICCV, pp. 433-438.

[2] Püspöki et al. (2016). Transforms and Operators for Directional Bioimage Analysis: A Survey. Advances in Anatomy, Embryology and Cell Biology, vol. 219(3): 69-93.

[3] Roseman (2003). Particle finding in electron micrographs using a fast local correlation algorithm. Ultramicroscopy, 94(3-4):225-236.

[4] Weber et al. (2012). Automated tracing of microtubules
in electron tomograms of plastic embedded samples of caenorhabditis elegans embryos Journal of Structural Biology, 178(2):129-138.

[5] Advani, Tucker (1987). The use of tensors to describe and predict fiber orientation in short fiber composites. Journal of Rheology, 31(8), 751.

[6] Bezrukov et al. (2006). Simulation and statistical analysis
of random packings of ellipsoids. Particle & Particle Systems Characterization, 23(5), 388-398.